Available online at www.sciencedirect.com
ScienceDirect
Trans. Nonferrous Met. Soc. China 23(2013) 567−575
Transactions of Nonferrous Metals Society of China
www.tnmsc.cn

Microstructure control of AZ31 alloy by self-inoculation method for semisolid rheocasting

Bo XING[1], Yuan HAO[1], Yuan-dong LI[1,2], Ying MA[1,2], Ti-jun CHEN[1,2]

1. State Key Laboratory of Gansu Advanced Nonferrous Metal Materials, Lanzhou University of Technology, Lanzhou 730050, China;
2. Key Laboratory of Nonferrous Metal Alloys and Processing, Ministry of Education, Lanzhou University of Technology, Lanzhou 730050, China

Received 9 December 2011; accepted 16 February 2012

Abstract: A novel rheocasting process, self-inoculation method (SIM), was developed for the microstructure control of semisolid wrought Mg alloy. This process involves mixing between liquid alloy and particles of solid alloy (self-inoculants), subsequently pouring the mixed melt into a special designed multi-stream fluid director. The primary phase with dendritic morphology in the conventionally cast AZ31 alloy has readily transformed into near spherical one in the slurry produced by SIM from melt treatment temperature between 690 °C and 710 °C and self-inoculants addition of 3%−7%. Achievement of the non-dendritic microstructure at the higher melt treatment temperature requires more self-inoculants addition or decreases in the slope angle of fluid director. Primary phase in the slurry thus produced has attained an ideally globular morphology after isothermal holding at 620 °C for 30 s. The increasing holding time leads to decrease of shape factor but the coarsening of particle size. The spheroidization and coarsening evolution process of solid particles during the isothermal holding were analyzed by Lifshitz-Slyozov-Wagner (LSW) theory.
Key words: AZ31 alloy; microstructure; semisolid rheocasting; self-inoculation method

1 Introduction

Wrought Mg alloys have widely varied applications in aerospace, automobile and electrical appliance industries because of their low density, high specific strength and stiffness [1]. The current technologies for wrought Mg alloy production are focused on solid deformation, such as forging, extrusion and rolling. However, these processes have to be carried out at a high temperature and low speed, resulting in a low productivity and high cost [2]. To cast these alloys directly into components has many economical advantages. The major problems encountered by conventionally casting are the poor castability of wrought alloys and the traditional cast defects [3]. Alternatively, semisolid casting is an idea technology in near-net shaping wrought Mg components because it offers great potential in reducing segregation and porosity, diminishing hot tearing, and improving mechanical properties [4−6].

Thixocasting and rheocasting are the two main technologies for fabrication of semisolid slurry. In recent years, rheocasting has aroused much attention due to its low cost and high productivity compared with thixocasting [7]. In order to realize rheocasting, the semisolid slurry with fine and spherical microstructure should be initially prepared during the solidification of alloy. During the past 30 years, several methods have been developed to produce the required microstructure. Alternatively, the methods based on nucleation enhancing mechanism are the simple and reliable options. The series of methods include new rheocasting (NRC) [8], semisolid rheocasting (SSR) [9], swirled enthalpy equilibration device (SEED) [10], and continuous rheoconvection process (CRP) [11]. Unfortunately, up to now, there has not been a published paper that reported the application of these processes in wrought Mg alloys.

In this work, a novel rheocasting process self-inoculation method (SIM), was developed for the

Foundation item: Project (2007CB613700) supported by the National Basic Research Program of China; Project (50964010) supported by the National Natural Science Foundation of China
Corresponding author: Yuan-dong LI; Tel: +86-931-2976795; E-mail: liyd_lut@163.com
DOI: 10.1016/S1003-6326(13)62501-7

non-dendritic slurry preparation. This process involves mixing between liquid alloy and particles of solid alloy (self-inoculants), and subsequently pouring the mixed metal into a special designed multi-stream fluid director. One of the widely used wrought Mg alloys, AZ31 alloy, was used as the experimental alloy. A series of casting trials were conducted to investigate the feasibility and necessary condition to achieve the refined and near spherical microstructure of AZ31 alloy by using SIM. Moreover, the microstructure evolution of primary α-Mg phase in the semisolid isothermal holding of slurry was investigated.

2 Experimental

Compositions of the used AZ31 alloy were (mass fraction): Al 3.1%, Zn 0.9%, Mn 0.3%, Mg balance. The liquidus temperature of this alloy is 634 °C. Figure 1 shows the solid fraction—temperature relationship and the temperature sensitivity of solid fraction of AZ31 alloy established by a commercial thermodynamic software package called Pandat on the basis of Scheil model. It can be seen that the temperature sensitivity of solid fraction, which is defined as $|\mathrm{d}f_s/\mathrm{d}T|$ [12], decreases with decreasing temperature or increasing solid fraction, except a slight increase that takes place at the eutectic temperature of 407 °C. It is generally claimed that 30%−50% solid is needed in the slurry for rheocasting. In the corresponding temperature range for the present alloy (approximately 624−618 °C), temperatures near 620 °C were selected to be the quenching temperatures for the followed experiments. The corresponding change in solid fraction with temperature was 0.024 and the solid fraction was 40%.

1 kg ingot of AZ31 alloy was melted in a steel crucible located at the electric resistance furnace. The molten alloy was degassed at 740 °C with 1% Cl_2C_6 and cooled down to a desired temperature (melt treatment temperature). Then, SIM process was operated, as shown in Fig. 2(a). A given amount of self-inoculants (addition amount) was added into melt, followed by hand stirring the melt in 5 s with a stainless rod. Then the mixed metal was poured and flowed equally down the fluid director with a settled slope angle. After pouring, the melt was collected in an accumulator at the exit of fluid director and cooled to a desired temperature. For self-inoculants preparation, as-cast ingot was transformed into particles using mechanical fragmentation. The maximum dimensions were 7 mm×7 mm×7 mm but without special morphology requirement. The fluid director (Fig. 2(b)) with 600 mm in length was a block of low carbon steel with two parallel channels divided by a shunting surface, and converged two-part way down the plate. The surface of fluid director was coated with ZnO and its underneath was cooled by water circulation.

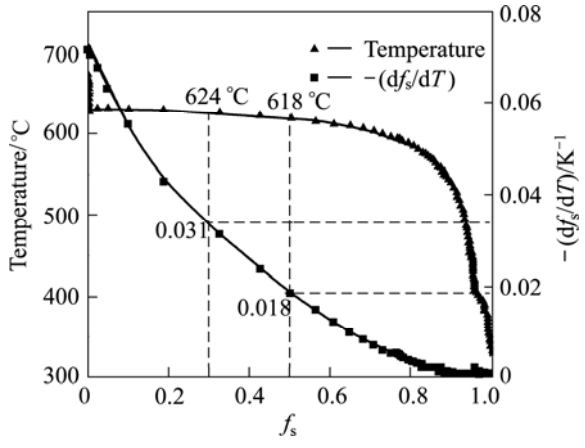

Fig. 1 Relationship between solid fraction (f_s) and sensitivity ($-\mathrm{d}f_s/\mathrm{d}T$), and processing temperature of AZ31 alloy

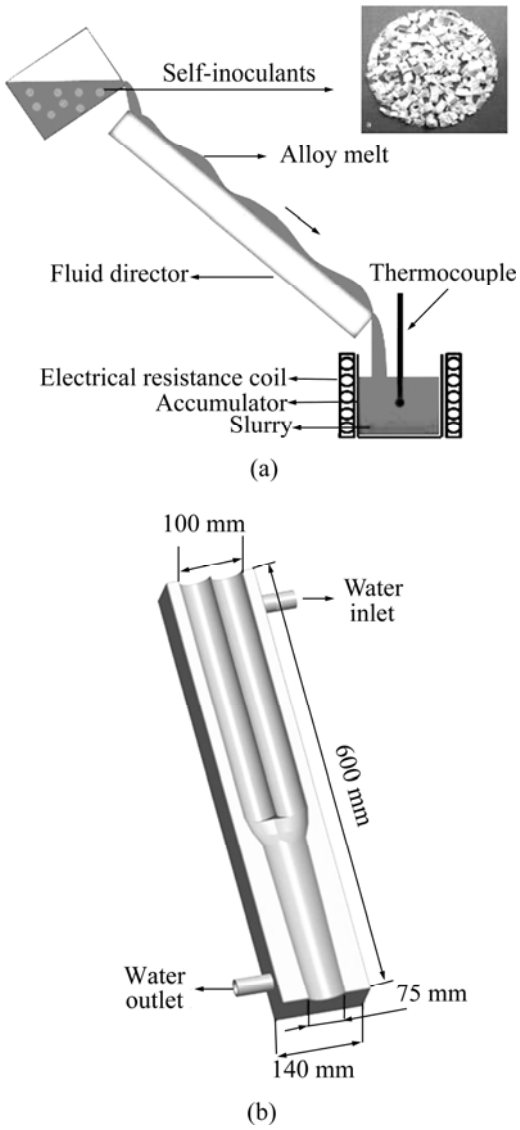

Fig. 2 Illustration of SIM process (a) and structure details of fluid director (b)

In this work, three process parameters, melt treatment temperature, addition amount of self-inoculants, slope angle of fluid director, were considered. It should be noted that when a parameter is varied, the others two parameters keep unchanged. Details of the experiment configurations are listed in Table 1. In each pouring, a 575 °C preheated stainless crucible of 80 mm in diameter and 120 mm in depth was placed at the exit of fluid director to cool the slurry with an average cooling rate of 0.56 °C/s. One K-type thermocouple was previously installed at the crucible center to record the change of slurry temperature. When the temperature reached (620±2) °C, the slurry was taken out and quickly quenched in cold water. For comparison, a melt was directly poured at 710 °C into the accumulator and quenched similarly.

Finally, in order to investigate the microstructure evolution of primary Mg phase in the isothermal holding, slurries produced at 710 °C with 5% self-inoculants addition were cooled to 620 °C and then held at this temperature for 30 s, 4 min, 15 min and 30 min and then quenched.

All specimens, produced from the center of quenched samples, were prepared by standard procedure and etched with 10% HCl aqueous solution. Microstructure feature was examined with a MeF3 optical microscope, quantitative analysis of solid particles was carried out using image analysis system. The circular diameter $D=2(A/\pi)^{1/2}$ and the shape factor $F=P^2/(4\pi A)$, where A and P are the average area of primary particles and average perimeter, respectively.

Table 1 Processing parameters of SIM used in this work

Melt treatment temperature/°C	Addition amount/%	Slope angle/(°)
690	3, 5, 7, 9	45
710	3, 5, 7, 9	45
735	3, 5, 7, 9	45
710	5	15, 30, 60
735	5	15, 30, 60

3 Results and discussion

3.1 Effect of melt treatment temperature and addition amount of self-inoculants on microstructure of AZ31 slurry under SIM

Figure 3 shows the semisolid microstructure of AZ31 alloy produced by conventionally casting at pouring temperature of 710 °C and cooling rate of 0.56 °C/s and then quenching at 620 °C. The white phase is primary α-Mg and the dark continuous matrix is the quenched liquid. It shows that the primary dendrites of the sample are very developed and most of the secondary dendritic arms are longer than 200 μm.

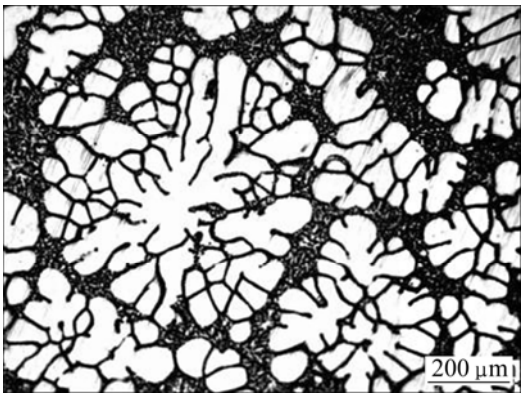

Fig. 3 Optical metallograph showing semisolid microstructure of AZ31 alloy produced from conventionally casting and quenching at 620 °C

Figure 4 shows the microstructure of slurries cast over SIM at 690 °C and various self-inoculants addition of 3%, 5%, 7% and 9%. A comparison of Figs. 3 and 4 reveals that the developed dendrites of α-Mg phase are changed into fine and nearly spherical particles by the application of SIM. From Figs. 4(a) and (b), it is evident that an increase in the addition of self-inoculants from 3% to 5% leads to a decrease in the size of α-Mg phase from 81 μm to 67 μm and an increase in shape factor from 1.58 to 1.84. A comparison of Figs. 4(b) and (c) reveals that more increase in the addition of self-inoculants from 5% to 7% leads to a slight decrease of primary α-Mg phase up to 61 μm and an increase in the shape factor from 1.84 to 1.91. However, by comparing Figs. 4(c) and (d), it is found that increasing addition to 9% leads to a visible increase of α-Mg phase size and the deterioration of particle morphology.

Figure 5 indicates the variations in solid particle size and shape factor of α-Mg phase with melt treatment temperature and addition amount of self-inoculants. It can be seen that the variations in particle size present a similar tendency to the superheat of 55 °C and 75 °C of melt, the particle size decreases with the increasing addition amount from 3% to 7% then a sharp increase occurs at the addition up to 9%. The shape factor increases with the increasing addition in these two cases. However, it is visible that an inverse tendency occurs when the 100 °C superheat was employed. In this condition, both the particle size and shape factor decrease with the increasing addition and the best value is obtained at 9%. Therefore, it can be concluded there are appropriate combinations between melt treatment temperature and self-inoculants addition. In order to produce large quantity of primary phase in melt with high superheat, more addition of solid particles is required.

According to the obtained results, grain multiplication in undercooled melt is the fundamental for

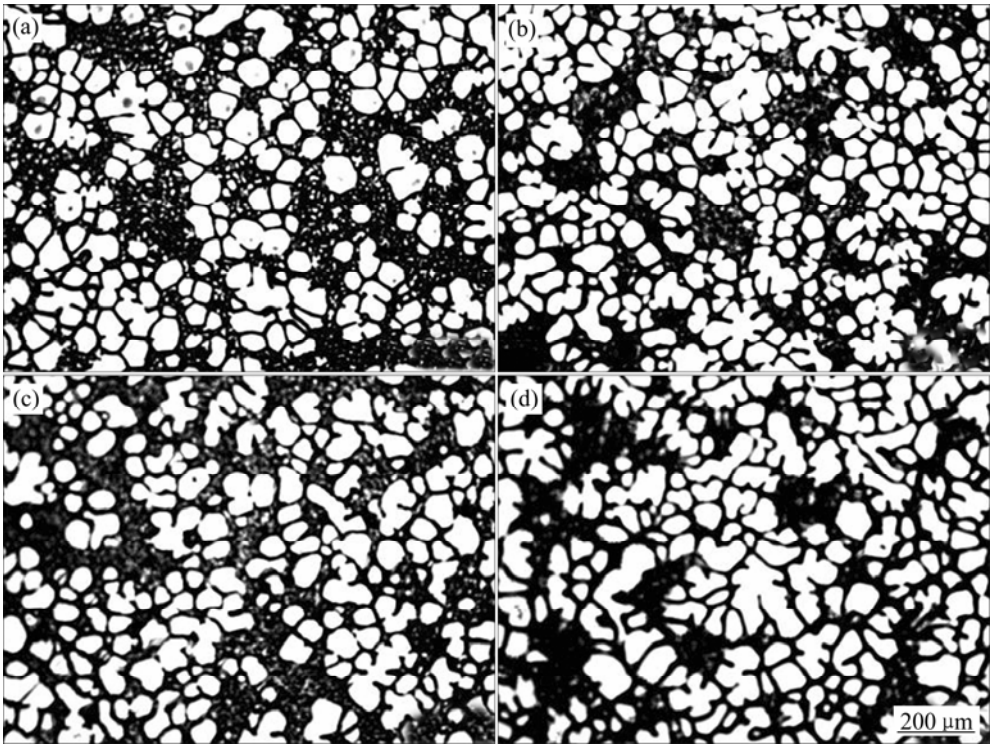

Fig. 4 Optical metallographs showing microstructures of AZ31 slurry produced by SIM at 690 °C with different addition amount of self-inoculants: (a) 3%; (b) 5%; (c) 7%; (d) 9%

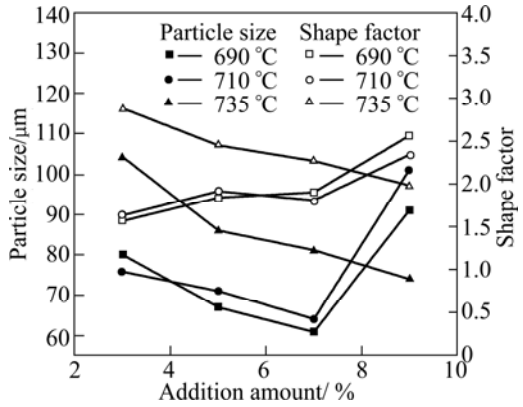

Fig. 5 Variation of primary particle size and shape factor with various melt treatment temperature and addition amount of self-inoculants

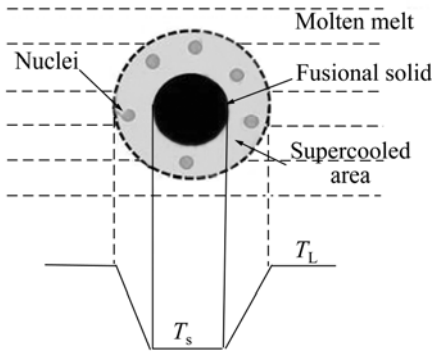

Fig. 6 Schematic diagram of temperature field around fusing solid

non-dendritic microstructure formation [13,14]. In SIM, the primary nucleation enhancement in alloy is achieved by the addition of self-inoculants. When the solid particles were immersed in melt with the identical composition, the intense heat transfer between solid and liquid generates strong temperature fluctuation in bulk melt. Consequently, mass of undercooled areas appears around the fusional solid particles [15], as shown in Fig. 6. In light of the transient nucleation theory proposed by STEFANESCU [16], the quasi-solid atom clusters in these areas have excellent wettability with nuclei, thus they can rapidly develop to free nucleus when their size reached the critical radius for heterogeneous nucleation. Moreover, according to study of XU et al [17], the melt produced by solid fusion contains a large number of dendrite fragments in the front of fusion interface resulting from the remelting of primary dendrites in solid alloy. These fragments also can serve as efficient nucleation substrate to precipitate to be primary phase and contribute to the grain multiplication.

Another resource of nuclei is the free crystals induced by fluid director. When the melt flows over fluid director, heterogeneous nucleation rapidly takes place on or near the plate surface. The liquid convection induced by fluid director leads to detachment of formed crystals from the plate surface [18] or the breaking of dendrites formed in the thermal undercooled region near the plate

wall [19]. Finally, these formed solid particles accompanied to melt flowing over the fluid director then were poured into the accumulator.

During the continuous cooling stage of the slurry, a controlled low cooling rate leads to sufficient diffusion of solute and latent heat in bulk melt; meanwhile the concentration gradient in the front of solid/liquid interface can be rapidly reduced because of the overlapping diffusion layers between neighboring grains [14]. In this condition, the preferential growth of grains was totally suppressed, so the increase in solid fraction by cooling was achieved by the ripening of all primary particles under the Gibbs-Thomson effect [20]. As a result, the refined and nearly spherical microstructure was readily obtained.

Therefore, the different microstructure features shown in Figs. 4 and 5 were probably attributed to the different nucleation and survival rates of primary phase under the interaction between melt treatment temperature and addition amount of self-inoculants. The high superheat plus less addition of solid particles leads to complete fusion of the solid, thus either the quasi-solid atom clusters or the dendrite fragments were unlikely to stably exist in the alloy melt, so the nucleation sites were relatively reduced. On the contrary, if the low superheat or excess solid addition was employed, the effective fusion of solids cannot take place. Solid shell forms heavily on surface of fluid director as a result of reduced fluidity of melt, hence the ideal semisolid slurry also cannot be obtained.

Another important phenomenon is that this interaction closely determines the melt temperature at the outlet of fluid director, accordingly affects the survival rate of primary phase in the accumulator. Figure 7 shows the outlet melt temperature under different combinations of melt treatment temperature and addition amount of solid particles. Combining Figs. 4 and 5, it appears that under the appropriate combination of the two

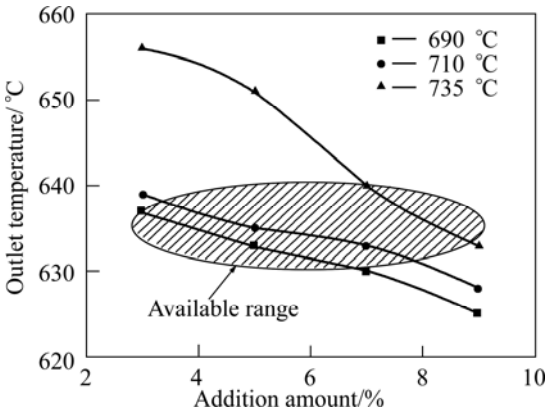

Fig. 7 Effect of interaction between melt treatment temperature and addition amount of self-inoculants on outlet temperature of melt in SIM

parameters, the outlet temperature of melt is near or below its liquidus and significant grain refinement can be obtained. This is consistent with the previous findings showed by MAO et al [21] that the low superheat of melt is beneficial for the crystals surviving, and thus promotes the globular microstructure formation.

3.2 Effect of slope angle of fluid director on microstructure of AZ31 slurry under SIM

Under the constant melt treatment temperature and self-inoculants addition, slope angle of fluid director is the main factor affecting the formation of free crystals in the flowing metal, finally determines the slurry microstructure. Figure 8 shows the microstructures of AZ31 slurry over SIM at 710 °C with 15°, 30°, 45°, 60° of fluid director. A comparison of Figs. 8(a) and (b) shows that the increase of the slope angle from 15° to 30° leads to elimination of dendritic microstructures. The small and nearly spherical particles were obtained when the angle was increased up to 45° or 60° .

Figure 9 indicates the variation of particle size and shape factor of α-Mg phase with the effect of slope angle and melt treatment temperature. It can be seen that when a relatively low temperature was employed, both the particle size and shape factor decrease with the increasing slope angle, the best value occurs at 45° and 60°. However, when the temperature of 735 °C was used, the variation of size and shape factor presents the inverse trendy. The angle between 15° and 30° was beneficial for the refined microstructure formation. Therefore, it is obvious that there also exist optimal angles for varied melt treatment temperature, which is required to transform the microstructure to a refined one.

The slope angle affects the heat extraction of alloy melt and the intense of shear stress applied to the chill crystals formed in metal flow. TAGHAVI and GHASSEMI [22] reported the formation of three layers within metal melt on the inclined plate that suffered from the different rates of heat transfer. The undercooled layer close to the plate surface is a solid layer containing chill crystals while the middle layer is a semisolid suspension layer containing liquid and dendrite fragments due to the perpendicular growth of primary phase towards plate surface. Increasing the angle up to 45° or 60° leads to the increase of intensity of shear stress and the shear strain. As a result, more solid particles were detached from the plate surface or were broken in the middle layer. Furthermore, under this condition, the heat transfer between the melt and plate surface increases as a result of decrease in the thickness of the bottom layer, and more chill crystals were formed into melt flowing over the plate. Finally, the fine and globular microstructures were produced, as shown in Figs. 8(c) and (d). This phenomenon has also been visually demonstrated in

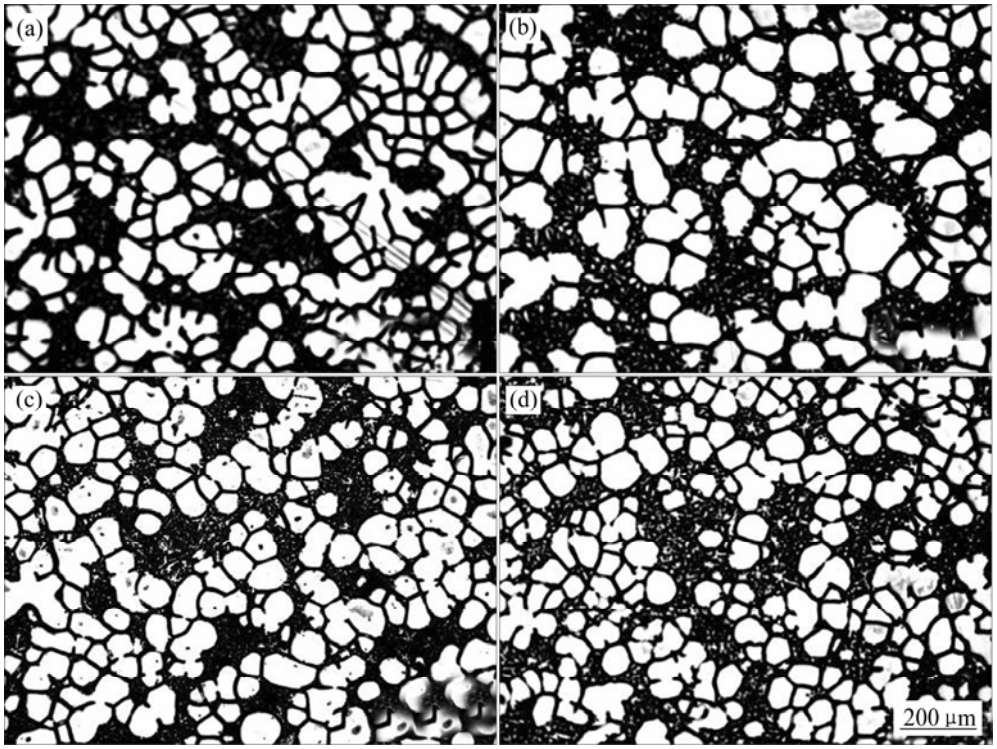

Fig. 8 Optical metallographs showing microstructures of AZ31 slurry produced by SIM at 710 °C with different slope angles of fluid director: (a) 15°; (b) 30°; (c) 45°; (d) 60°

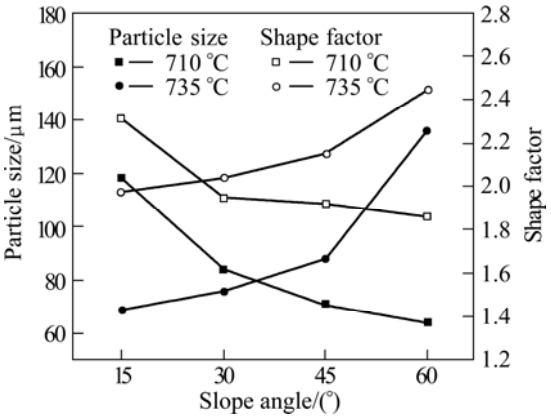

Fig. 9 Variation of primary particle size and shape factor in various melt treatment temperature and slope angle of fluid director

investigation by LEGORETTA et al [23] with a transparent analogue.

The duration time of heat transfer between melt and fluid director also depended on the slope angle. When the melt treatment temperature was low, the decrease of the slope angle led to excess long heat extraction time of the melt. Thus the thickness of supercooled layer was rapidly increased till the melt totally solidified on plate surface. Therefore, both the chill crystals and dendritic fragments were difficult to form in metal flow. As a result, the coarse microstructures formed, as shown in Figs. 8(a) and (b). However, when the melt treatment temperature was high, there was prolonged heat extraction time for metal melt if the low slope angles were employed, thus the nucleation rate can be relatively enhanced. Unfortunately, in such condition the shear stress exerted on solid particles was relatively small, thus the shape factor of particle was totally high, as shown in Fig. 9.

3.3 Microstructure evolution of AZ31 slurry during semisolid isothermal holding

In practical rheocasting, the semisolid slurry is usually handled isothermally prior to subsequent component shaping to adjust the morphology of primary phase and the solid fraction of slurry. Therefore, to get better understanding of solid particles evolution in the isothermal state is important because it determines the flow behavior of slurry and the final grain size of components, and thus mechanical properties.

Figure 10 shows the morphological evolution of α-Mg particles of AZ31 slurry during isothermal holding at 620 °C for different duration time. It is found in Fig. 9(a) that the microstructure is a mixture of ripened dendrite fragments, irregular polygons and some globular particles during the initial period of holding (30 s). With the increase of holding time, the protuberances on grain surface were gradually faded and all of the particles present in ideal spheroid. With the increasing holding time from 30 s to 30 min, the shape factor of primary phase decreases from 1.72 to 1.15 while the particle size increases from 58 to 172 μm. It is also visible that the

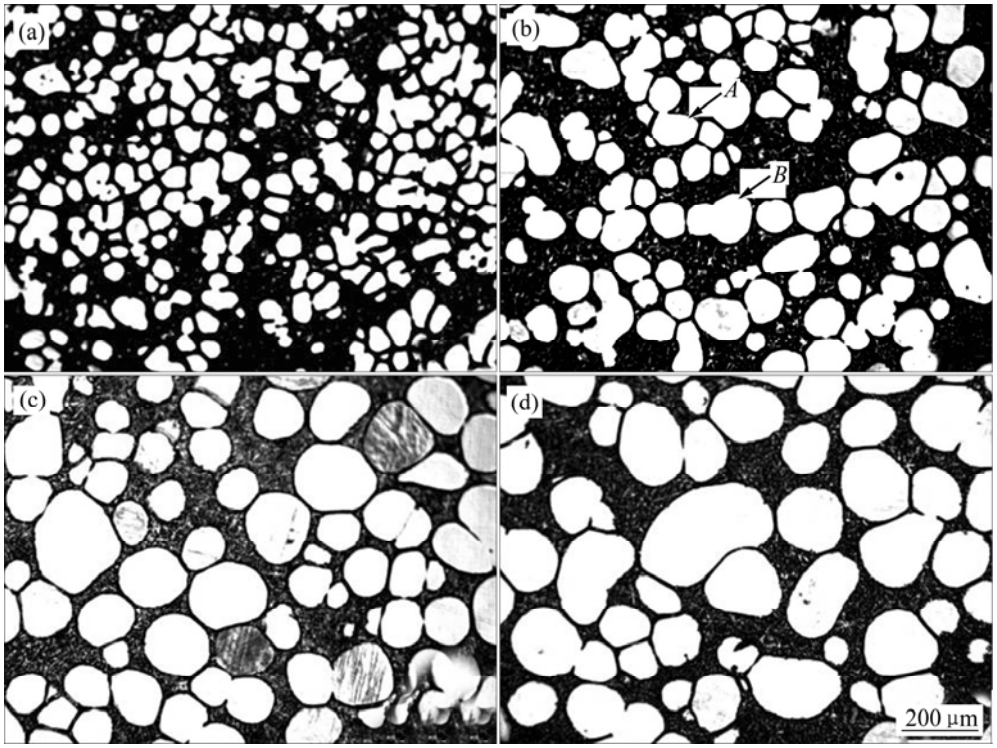

Fig. 10 Optical metallographs showing microstructures of AZ31 slurry produced by SIM after isothermal holding at 620 °C for 30 s (a), 4 min (b), 15 min (c) and 30 min (d)

number of α-Mg particles was gradually reduced with the prolonged holding time, and there as no entrapped eutectic within solid particles at different stages.

Generally, the microstructure evolution of semisolid alloy in the quiescent state is a result of solute diffusion dominated by the temperature and interfacial tension. In the present case, the slurry temperature was kept constant in whole process. So the growth and coarsening of primary particles can be treated as a spontaneous process mainly governed by the action of interfacial tension.

As shown in Figs. 4 and 8, the initial microstructure produced by SIM was a mixture of elliptical or near-spherical particles and the dendrite fragments. According to the thermodynamics in solidification, under the interfacial tension of S/L interface, the relationship between equilibrium melting point and the curvature of solid interface can be represented as [24]

$$\Delta T_{\mathrm{r}} = -\frac{2\sigma T_{\mathrm{p}} V_{\mathrm{s}}}{\Delta H_{\mathrm{m}}} k_{\mathrm{sl}} \tag{1}$$

where σ is the S/L interfacial tension; T_{p} is the melting point of plane interface; V_{s} is the molar volume of solid phase; ΔH_{m} is the change of molar enthalpy when the solid-liquid transformation happens; K_{sl} is the curvature of S/L interface.

It can be easily concluded from Eq. (1) that if there is an obviously projected part on the surface of solid particles, its melting point will be reduced as the function of interfacial curvature. Therefore, at the initial stage of isothermal holding, the projected part of α-Mg particles will be melted down and become liquid alloy due to the reduction of melting point caused by interface curvature. Consequently, the solid particles will gradually sphere and become regular in morphology, as shown in Fig. 10(a).

During the prolonged isothermal holding, the α-Mg particles undergo further coarsening under the mechanism of coalescence and Ostwald ripening. Generally, this process can be better analyzed using the classical LSW relationship expressed as [25,26]

$$D^n - D_0^n = Kt \tag{2}$$

where D_0 is the initial particle size; D is the particle size at time t; K is the coarsening rate constant; n is the coarsening exponent, and generally, equals 3 for volume-diffusion-controlled coarsening. The experiment data in Fig. 10 were reconstructed according to Eq. (2) at n=3 and the result is shown in Fig. 11. The R^2 value is close to 1, indicating that the experimental data are well fitted to the LSW equation at n=3. The average K value of 1410 μm^3/s is estimated for the whole isothermal heat treatment, the coarsening rate is much higher in the early stages as inferred from the higher initial slope of the curve. It is thus claimed that coarsening first proceeds predominantly through coalescence of particles which have perfectly matching crystallographic orientation.

This phenomenon can be visualized in Fig. 10(b) where arrow *A* indicates the coalescence of at least two connecting particles and arrow *B* shows the well coarsened grains.

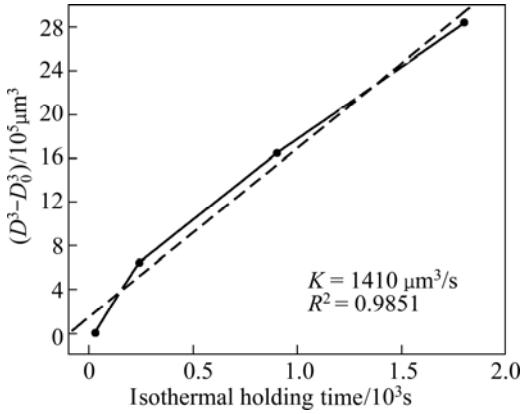

Fig. 11 Variation of cube of particle size of AZ31 alloy with isothermal holding time at 620 °C

While the coalescence dominates in the early stage, Ostwald ripening seems to be the dominant mechanism in the later stage. Under the driving force provided by the interface energy, small globules tend to melt, while larger ones tend to grow with the increasing holding time. Evidence for this mechanism is available from Figs. 10(c) and (d) that some of the small particles disappeared, meantime, the large particles underwent further coarsening. Due to the fact that an average grain size below 100 μm is available for the rheocasting operation, the critical time of isothermal holding of 10 min, can be acceptable under the present condition.

4 Conclusions

1) The semisolid slurry of AZ31 alloy with fine and nearly spherical solid particles was prepared by the self-inoculation method. The interaction between melt treatment temperature and addition amount of self-inoculants has great influence on the morphology and size of primary α-Mg phase. The optimum processing range is suggested as follows: melt treatment temperature is between 690 and 710 °C and self-inoculants addition is between 3% and 7%.

2) The slope angle between 45° and 60° is beneficial to the non-dendritic primary phase formation at the low melt temperature; in order to obtain the refined microstructure at the relatively high melt treatment temperature, the slope angle between 15° and 30° is required.

3) The irregular morphology of primary α-Mg phase in SIM slurry is changed to an ideally globular structure during the isothermal holding of slurry at 620 °C. Excessive long holding time leads to coarsening of primary α-Mg phase without visible change in the globularity. Coalescence is most likely the dominant grain growth mechanism in the early stage of isothermal holding while Ostwald ripening tends to be the principal one in the later stage.

References

[1] POLMEAR I J. Magnesium alloys and their applications [J]. Materials Science and Technology, 1994, 10(1): 1−16.

[2] ZHANG S M, FAN Z, ZHEN Z. Direct chill rheocasting (DCRC) of AZ31 Mg alloy [J]. Materials Science and Technology, 2006, 22(12): 1489−1498.

[3] GUO H M, YANG X J. Preparation of semi-solid slurry containing fine and globular particles for wrought aluminum alloy 2024 [J]. Transactions of Nonferrous Metals Society of China, 2007, 17(4): 799−804.

[4] FLEMINGS M C. Behavior of metal alloys in the semi-solid state [J]. Metallurgical and Materials Transaction A, 1991, 22(5): 957−981.

[5] JI Z S, HU M L, SUGIYAMA S, YANAGIMOTO J. Formation process of AZ31B semi-solid microstructures through strain-induced melt activation method [J]. Materials Characterization, 2008, 59: 905−911.

[6] GUAN R G, ZHAO Z Y, SUN X P, HUANG H Q, DAI C G, ZHANG Q S. Fabrication of AZ31 alloy wire by continuous semisolid extrusion process [J]. Transactions of Nonferrous Metals Society of China, 2010, 20(s3): s729−s733.

[7] SIM J G, CHOI B H, JANG Y S, KIM J M, HONG C P. Development of a nucleation-accelerated-semisolid-slurry-making method and its application to rheo-diecasting of ADC10 alloy [J]. ISIJ International, 2010, 50(8): 1165−1174.

[8] KAUHANN H, WABUSSEG H, UGGOWITZER P J. Metallurgical and processing aspects of the NRC semi-solid casting technology [J]. Aluminum, 2000, 76(1−2): 70−75.

[9] MARTINEZ R A, FLEMINGS M C. Evolution of particle morphology in semisolid processing [J]. Metall Mater Trans A, 2005, 36: 2205−2210.

[10] TEBIB M, MORIN J B, AJERSCH F, CHEN X G. Semi-solid processing of hypereutectic A390 alloys using novel rheoforming process [J]. Transactions of Nonferrous Metals Society of China, 2010, 20(9): 1743−1748.

[11] FINDO M, APELIAN D. Continuous rheoconversion process for semi-solid slurry production [J]. Transactions of the American Foundry Society, 2004, 112: 305−323.

[12] LI Y D, APELIAN D, XING B, MA Y, HAO Y. Commercial AM60 alloy for semisolid processing: I. Alloy optimization and thermodynamic analysis [J]. Transactions of Nonferrous Metals Society of China, 2010, 20(9): 1572−1578.

[13] MARTINEZ R A. Formation and processing of rheocast microstructure [D]. Boston: Massachusetts Institute of Technology, 2004: 26−52.

[14] GUO Hong-min, YANG Xiang-jie. Formation mechanism of spherical particles in undercooled melt [J]. The Chinese Journal of Nonferrous Metals, 2008, 18(4): 651−659. (in Chinese)

[15] MA Yu-tao, ZHANG Xing-guo, HAO Hao, WANG Yun-bo, JIN Jun-ze. Effects of CaC_2 on microstructure and tensile properties of AZ61 magnesium alloys by electromagnetic-suspension casting [J]. The Chinese Journal of Nonferrous Metals, 2009, 19(3): 445−451. (in Chinese)

[16] LU Gui-min, DONG Jie, CUI Jian-zhong, CHANG Shou-wei. As-cast microstructures and the solidifying mechanism of 7075 alunminum alloy cast by LSC [J]. Acta Metallurgica Sinica, 2001, 37(10): 1045−1048. (in Chinese)

[17] XU D M, PEHIKE R D, LI Q C. Melting interface morphology of Al−4%Cu, eutectic Al−Cu and Al−Si alloy [J]. AFS Transactions, 1992, 100: 961−968.
[18] OHNO A. Solidification—The separation theory and its practical applications [M]. Berlin: Springer-Verlag Press, 1987.
[19] GUAN R G, CAO F R, CHEN L Q, LI J P, WANG C. Dynamical solidification behaviors and microstructural evolution during vibrating wavelike sloping plate process [J]. Journal of Materials Processing Technology, 2009, 209: 2592−2601.
[20] GUO H M, YANG X J. Efficient refinement of spherical grains by LSPSF rheocasting process [J]. Materials Science and Technology, 2008, 24(1): 55−61.
[21] MAO W M, CUI C L, ZHAO A M, YANG J L, ZHOGN X Y. Effect of pouring process on the microstructure of semi-solid $AlSi_7Mg$ alloy [J]. Journal of Materials Sciences and Technology, 2001, 17(6): 615−619.
[22] TAGHAVI F, GHASSEMI A. Study on the effects of the length and angle of inclined plate on the thixotropic microstructure of A356 aluminum alloy [J]. Materials and Design, 2009, 30: 1762−1767.
[23] LEGORETTA E C, ATKINSON H V, JONES H. Cooling slope casting to obtain thixotropic feedstock I: Observations with a transparent analogue [J]. Journal of Material Science, 2008, 43: 5448−5455.
[24] HU Han-qi. Metal solidification [M]. Beijing: Metallurgical Industry Press, 1985: 245. (in Chinese)
[25] LIFSHITS I M, SLYOZOV V V. Kinetics of precipitation from supersaturated solid solutions [J]. J Phys Chem Solids, 1961, 19: 35−50.
[26] AGNER C. Theory of aging from precipitation by Ostwald ripening [J]. Z Electrochem, 1961, 65(7−8): 581−586.

自孕育法制备 AZ31 镁合金半固态流变成形组织

邢 博[1]，郝 远[1]，李元东[1,2]，马 颖[1,2]，陈体军[1,2]

1. 兰州理工大学 甘肃省有色金属新材料省部共建国家重点实验室培育基地，兰州 730050；
2. 兰州理工大大学 有色金属合金及加工教育部重点实验室，兰州 730050

摘 要：采用新型自孕育流变铸造技术对变形镁合金半固态组织进行控制。该工艺过程为将合金熔体与一定量的合金固体颗粒(自孕育剂)混合，然后将混合金属通过一个多流股导流器浇入铸型或收集器。结果表明：采用自孕育工艺，合金熔体处理温度 690~710 °C，孕育剂的加入量为 3%~7%时能有效将 AZ31 镁合金传统铸造中的粗大枝晶组织转变为细小、近球状的非枝晶组织；当合金熔体处理温度较高时，增加孕育剂的加入量或减小导流器的倾斜角度有利于获得非枝晶组织。自孕育工艺制备的 AZ31 镁合金半固态浆料在 620 °C 等温保温 30 s 后能有效改善初生 α-Mg 颗粒的圆整度；延长保温时间有助于减小颗粒的圆整度，但同时颗粒发生粗化。利用 Lifshitz-Slyozov-Wagner (LSW)理论对初生相颗粒在等温保温过程中的组织圆整、粗化过程进行了分析。

关键词：AZ31 合金；微观组织；半固态流变成形；自孕育工艺

(Edited by Hua YANG)